Available online at www.sciencedirect.com

ScienceDirect

Energy Procedia 55 (2014) 777 – 785

Energy Procedia

4th International Conference on Silicon Photovoltaics, SiliconPV 2014

MF-sputtered AZO for a-Si SHJ solar cells

Jan Jeurink[a,*], Florian Wagner[a], Sunah Park[a], Laurent Kroely[a], Winfried Wolke[a]

[a]*Fraunhofer Institute for Solar Energy Systems, Heidenhofstr. 2, 79110 Freiburg, Germany*

Abstract

Silicon Hetero Junction (SHJ) structures and ZnO:Al (AZO) were deposited completely by high throughput industrial inline CVD and PVD deposition systems, respectively. A design of experiment of the AZO deposition parameters was carried out, to find suitable AZO layers for the use in SHJ solar cells. A subsequential thermal treatment on the AZO layers was performed to investigate their performance in a solar cell production. Thin AZO layers with the lowest specific resistance of 0.69 10^{-3} Ωcm were achieved with low *T* annealing. The highest carrier mobility of 22 cm^2 V^{-1} s^{-1} was reached with high temperature annealing.

Peer-review under responsibility of the scientific committee of the SiliconPV 2014 conference

Keywords: transparent conductive oxide; ZnO:Al; silicon heterojunction

1. Motivation

The use of ZnO:Al (AZO) for Silicon Hetero Junction (SHJ) solar cells as transparent conductive oxide (TCO) layer provides a highly available low cost alternative compared to indium based TCO's. The deposition was performed in an inline PVD system. The biggest disadvantage of thin AZO layers is its low carrier mobility μ (μ_{AZO} = 15 cm^2 V^{-1} s^{-1} [1], μ_{ITO} = 50 cm^2 V^{-1} s^{-1} [2]), which requires a high carrier concentration *N* to attain a low sheet resistance. A high *N* again results in higher free carrier absorption (FCA) of infrared light [3] and thereby to a reduced short circuit current density (J_{sc}) of a solar cell. Therefore the AZO deposition parameters were varied to obtain a high carrier mobility of AZO. As known from literature, a post thermal treatment can be beneficial for AZO [1] and was therefore investigated for bare AZO layers and a-Si SHJ lifetime samples.

* Corresponding author. Tel.: +49-761-4588-5964; fax: +49-761-4588-7812.
E-mail address: jan.jeurink@ise.fraunhofer.de

Peer-review under responsibility of the scientific committee of the SiliconPV 2014 conference
doi:10.1016/j.egypro.2014.08.059

2. Experimental

The AZO layers were deposited by an inline sputtering system from Applied Materials (ATON 500), with a dual magnetron at medium frequency (MF). The planar ZnO sputtering target contains 2 weight% aluminum and the sputtering gas is argon. The sample substrates are placed on a carrier plate and locked in the vacuum system. Within the vacuum system the substrates are heated up to the process temperature and pass through the plasma region, where the deposition takes place. The carrier speed determines the resulting AZO layer thickness, which was kept constant at ca. 70 nm, controlled by ellipsometry measurements on shiny-etched crystalline silicon (c-Si) samples. The process parameters, the electrical power of the sputtering system P, the deposition temperature T and the Argon flux [Ar], were varied according to a statistical design of experiment (DoE), as shown in Table 1. The concentration N and the effective mobility μ of the charge carriers were obtained by hall measurements [4] with AZO films on bare glass or on a-Si coated glass substrates. Annealing was carried out subsequentially either in a furnace with controlled gas atmosphere or on a hotplate in air. From the annealing temperature T_{ann} dependent carrier concentration N, the donor activation energy E_a through the Arrhenius equation [5] can be estimated:

$$\ln(N) = \frac{-E_a}{R}\frac{1}{T_{ann}} + \ln(A), \tag{1}$$

with R as the ideal gas constant and the pre factor A, which is independent from N. Symmetrical amorphous silicon hetero junction layers on shiny-etched c-Si wafers were used to investigate the effect of AZO deposition and post annealing on the potential cell performance. The samples were characterized by quasi steady state photo conductance (QSSPC) method [6] to get the implied pseudo fill factor *i-pFF* [7] and the implied open circuit voltage *i-*V_{oc} [8].

Table 1. Process parameters of the MF-sputtered ZnO:Al layers.

Factors	Range
Power P (kW)	5 – 13
Deposition temperature T (°C)	25 – 300
Argon flux [Ar] (sccm)	200 – 500

3. Results

3.1. Design of Experiment (DoE)

The analysis of variance resulting from the DoE of the AZO deposition is shown in Fig. 1 (a). The significance level is set to a probability p of 0.005. At a low argon flux of 200 sccm, no significant effect of the deposition parameters on the carrier mobility μ and concentration N was observed. At the higher argon flux of 500 sccm, the temperature becomes a significant parameter for the N and μ. The detailed effect of the deposition temperature on μ and N for high argon flux is shown in Fig. 1 (b). Primarily the mobility μ increases for higher deposition temperature T, whereas the carrier concentration N decreases. For a too high deposition temperature, however, the mobility decreases and the concentration increases again. The hypothesis for low temperature AZO is probably a higher micro structure, e.g. smaller and therefore more grains, which causes a higher defect density at the grain boundaries [9] with donor like behavior. The more grains again can explain the very low mobility of below 10 $cm^2V^{-1}s^{-1}$, since it is known that the grain-to-grain mobility in AZO is very low due to scattering effects at the grain interfaces and therefore the limiting factor of the effective mobility [9]. The microstructure of AZO deposited at higher temperatures is probably reduced, which would result in a lower grain boundary defect induced carrier concentration but a higher carrier mobility due to less grain-to-grain transfers. The increase of the carrier concentration for AZO deposited at 300 °C can be explained by an in-situ thermal activation of donors.

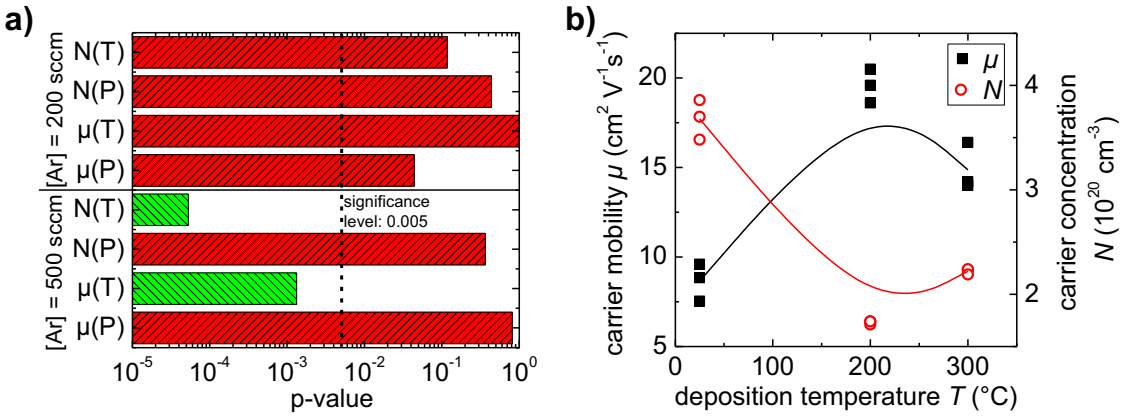

Fig. 1. (a) Significance test of the AZO deposition parameter (see Table 1) on the carrier concentration and carrier mobility of the AZO film, (b) effect of the deposition temperature T on the carrier mobility μ and concentration N of AZO deposited at an Argon flux of 500 sccm.

3.2. Structural and optical properties of AZO

In Fig. 2 SEM pictures of AZO deposited at 200 °C with an argon flux of 500 sccm on a-Si coated c-Si wafers are shown. The deposition of the thick layer in picture (a) was performed with a slower deposition speed. The 1,3 µm thick AZO layer on a flat surface obtains a small grain incubation layer of roughly 80 nm. For a layer thickness greater 80 nm, the grain size increases. In picture (b) the thin AZO layer on an alkaline textured silicon surface shows the same small grain structure as the incubation layer in picture (a). The grain size of the thin AZO layer was estimated to 50 nm. The comparison of the electrical properties of the thick and thin AZO layers shows a difference in the carrier mobility μ and concentration N (see Table 2). The higher value for μ for the thick layer can be explained by the bigger grain size, since it is known that the in-grain mobility of AZO is dominantly limited by scattering effects with impurity ions [10] can be rather high [11]. For the small grain material, the carriers have to cross the grain boundaries more often, reducing the effective mobility due to scattering effects at the grain boundaries [10]. The higher carrier concentration of the thick AZO layer is probably due to a thermal activation of donors; due to the long plasma process, the time of the sample within the high temperature region is longer.

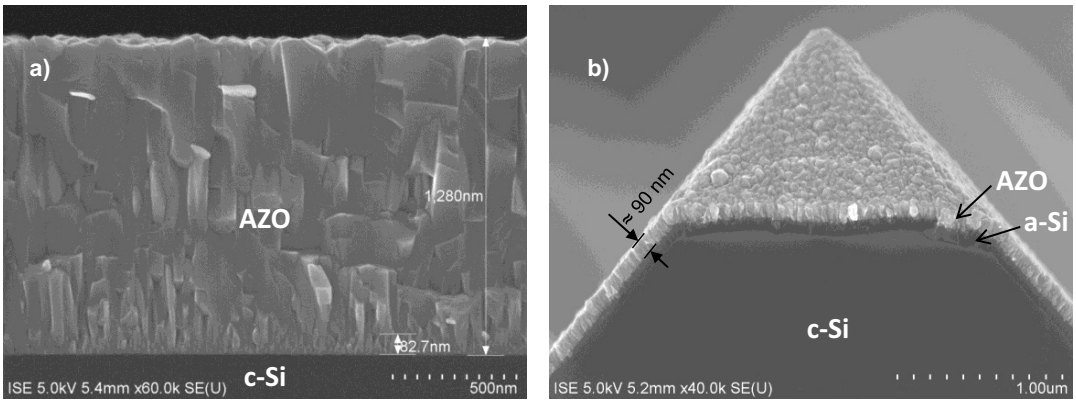

Fig. 2. SEM pictures of AZO deposited at 200 °C with an argon flux of 500 sccm (a) on a flat c-Si surface with a thickness of 1,3 µm and (b) on a random pyramids textured c-Si surface with a thickness of 90 nm. Both c-Si surfaces were covered with a-Si.

Table 2. Electrical comparison by Hall-measurements of thick and thin AZO layers deposited at 200 °C and 500 sccm argon flux on glass substrates.

Parameter	1,3 µm AZO	80 nm AZO
Specific resistivity ρ (Ω cm)	$0{,}5 * 10^{-3}$	$1{,}2 * 10^{-3}$
Carrier mobility μ ($cm^2 V^{-1} s^{-1}$)	28	20
Carrier concentration N (cm^{-3})	$4{,}3 * 10^{20}$	$2{,}4 * 10^{20}$

In Fig. 3 the extinction coefficient k of AZO layers deposited on glass with three carrier concentrations in the visible and near infrared wavelength range is shown. The carrier concentration N of the layers were obtained by Hall-measurements and the extinction coefficient was calculated from transmission and reflection measurements of AZO layers deposited on glass substrates. High carrier concentration causes High infrared light absorption which results in a lower short circuit current density J_{sc} of a SHJ solar cell, contacted by such an AZO layer. In Table 3, the J_{sc} loss due to light absorption within the AZO layers from Fig. 3, calculated with OPAL [12], is shown. The increase of the J_{sc} loss was found proportional to N^2.

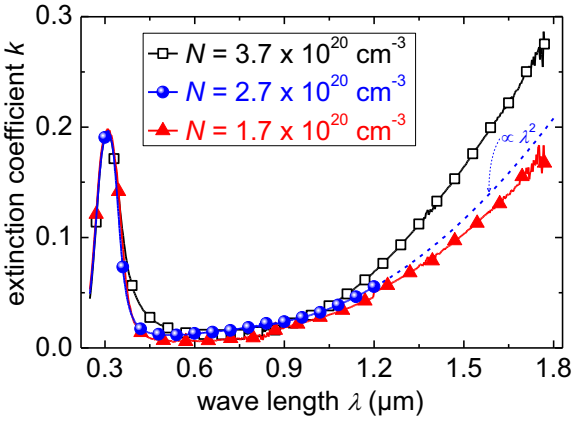

Fig. 3. Extinction coefficient k in the visible and near infrared wave length range for three AZO layers with different carrier concentrations N.

Table 3. Calculated J_{sc} loss due to light absorption within three AZO layers of 75 nm thickness with different carrier concentrations N, calculated with OPAL [12].

N (cm^{-3})	J_{sc} loss ($mAcm^{-2}$)
1.7×10^{20}	3,59
2.7×10^{20}	3,91
3.7×10^{20}	4,77

3.3. Annealing behavior of AZO

In Fig. 4 a-b) the time dependent annealing behavior of μ and N of AZO layers deposited on glass with an argon flux of 500 sccm and a sputtering power of 13 kW at different temperatures is shown. The annealing was carried out in nitrogen atmosphere subsequentially at 275 °C, except the very right points, where the temperature was raised up to 450 °C and the heating time was 30 min. The detailed effects are explained in the following sub sections.

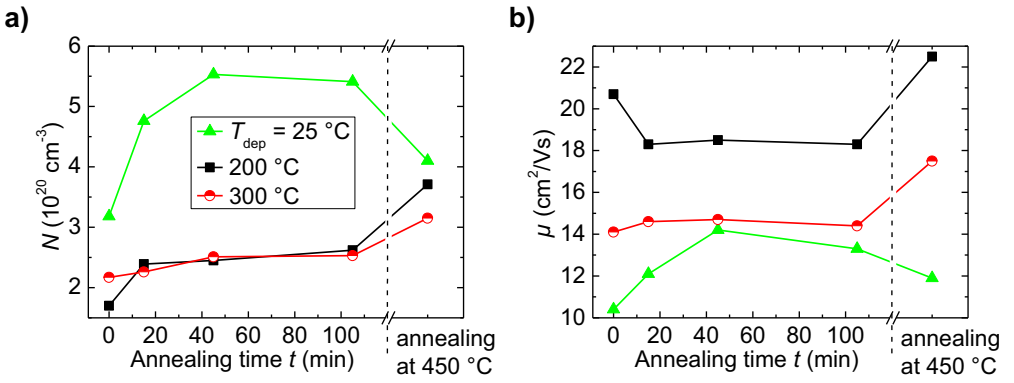

Fig. 4. Annealing time dependence of (a) the carrier mobility μ and (b) concentration N of AZO deposited on glass with an Argon flux of 500 sccm and a sputter power of 13 kW at different temperatures. The annealing temperature was 275 °C, except the very right points, which were annealed for 30 min at 450 °C. The annealing was carried out in nitrogen atmosphere.

3.3.1. Low T annealing at 275 °C

3.3.1.1. Behavior of N

Overall, an increase of the carrier concentration N for 275 °C annealing temperature for all AZO layers can be seen. Furthermore, the increase of N saturates with time, which can be explained by the thermal equilibrium of donor states. A more detailed look on the amount of the increase of N shows a dependence to the deposition temperature (see Fig. 4 a). By plotting the annealing temperature dependent change in the carrier concentration N before annealing and after the 100 min annealing at 275 °C in an Arrhenius graph, which is not shown here, one can estimate the activation energy E_a of the carrier formation. It becomes apparent that E_a for the 25 °C and 200 °C AZO amounts around 25 meV, whereas the 300 °C AZO shows a smaller increase of the carrier concentration with an activation energy of around 10 meV. An assumption for this behavior is an already reached thermal equilibrium of the donor formation for AZO deposited at 300 °C, due to the in-situ annealing during sputtering, whereas the 25 °C and 200 °C AZO reach the thermal equilibrium of the donor activation with annealing due to the lower deposition temperature.

3.3.1.2. Behavior of μ

The annealing behavior of the carrier mobility μ shows also a strong dependence on the deposition temperature of the AZO layers (see Fig. 4 b). Whereas the low temperature AZO benefits by a thermal treatment up to 275 °C, the 200 °C AZO suffers. One can assume the improvement of μ for the low temperature AZO is linked to structural improvements of the layer, however, these structural properties still limiting the mobility on a lower level. The higher mobility of the 200 °C AZO is probably limited not only by structural but also by in-grain ion scattering effects, which depends on the carrier concentration and results therefore in a decreasing μ, since N increases. The mobility of the 300 °C AZO again remains more or less constant, as the carrier concentration is also not changed.

3.3.2. High temperature annealing at 450 °C

3.3.2.1. Behavior of N and μ

The high temperature annealing at 450 °C in contrast obtains a different behavior. The low temperature AZO seems to be dominated by as-deposited structural properties which leads to a decrease of N, probably due to a saturation of e.g. grain boundary defects. That this effect appears only at high temperature annealing is probably due to the higher thermal energy, which is required for the restructuring of the layer. The deterioration of the carrier mobility, however, cannot be explained by this hypothesis and is obviously limited by other built-in scattering effects. In the case of 200 °C and 300 °C AZO, a thermal treatment of 450 °C leads to an increasing carrier

concentration with a specific donor activation energy of around 55 meV, which is found in the literature as a formation of Al_{Zn} donors [13]. The strong increase of the mobility for the high temperature AZO layers is in contradiction to the increase of N, since a higher ion scattering and therefore a reduced mobility is predicted. Therefore other mechanisms, as e.g. lower neutral impurity scattering or scattering at crystallographic defects [14], seems to play a significant role. However, a similar effect was shown by Ruske et al. [14], where the carrier mobility of bulk AZO reached values up to 65 $cm^2V^1s^{-1}$ with an even higher carrier concentration after a long thermal treatment at 650 °C. It can be pointed out, that AZO layers deposited at temperatures below the annealing temperature shows a huge modification with the post deposition thermal treatment. Nonetheless long annealing at 450 °C is too high for a-Si SHJ solar cells, the information that there is an improvement of the electrical parameters of AZO by applying certain energy can be useful for e.g. very short thermal treatments.

3.3.3. AZO on SHJ structures

In Fig. 5 (a) and (b) the effects of a subsequential annealing for 15 minutes at different temperatures on the implied pseudo fill factor (*i-pFF*) and the implied open circuit voltage (*i-*V_{oc}) of (a) AZO/a-Si:H(n-i)/c-Si(n)/a-Si:H(i-n)/AZO hetero BSF and (b) AZO/a-S:H(p-i)/c-Si(n)/a-Si:H(i-p)/AZO hetero emitter structures are shown. The thickness of the a-Si stacks and AZO layers was 20 and 80 nm, respectively. The AZO deposition temperature was 200 °C with an argon flux of 500 sccm and a power of 13 kW. For both structures a decrease of the *i-pFF* after AZO deposition was observed, whereas the *i-*V_{oc} stays more or less constant. The degradation of *i-pFF* after AZO deposition can be explained by the high energy radiation during the sputtering process. The different behavior of *i-pFF* and *i-*V_{oc} is due to the different injection level of minority carriers for the estimation of *i-pFF* and *i-*V_{oc}. Whereas *i-pFF* is estimated at a minority carrier density (MCD) of around 1 x 10^{15} cm^{-3}, the *i-*V_{oc} is calculated at 1 sun radiation, which is our case a MCD of around 1 x 10^{16} cm^{-3}. In the high MCD range the carrier lifetime is dominantly limited by the Auger recombination, which is not altered by the sputter deposition. In the lower MCD range, the so called Shockley-Read-Hall (SRH) recombination takes place, which is highly increased by the defect formation due to the high energy radiation during the sputtering process. The subsequential post annealing obtains an improvement of the sputter degraded *i-pFF* up to a temperature of 275 °C. The *i-*V_{oc} shows an improvement up to a temperature of 275 °C. A higher temperature treatment causes a degradation of both parameters for BSF and emitter structures. Hall measurements of AZO on such SHJ structures indicates a larger carrier concentration N for AZO deposited on a-Si surfaces and strong increase of N for annealing up to 300 °C (Fig. 5 d). The energy for the donor activation in the temperature range from 250 to 300 °C is independent from the underlying layers, but the comparison between AZO on glass and a-Si stacks shows different degradation mechanisms. Whereas the bare AZO starts to deteriorate at 325 °C, the AZO on a-Si(i-p) is especially stable up to 350 °C. These differences of μ and N, and the changed thermal behavior can be due to either a different surface morphology, which can lead to a different structure of AZO, or to an allocation of hydrogen during the AZO deposition in cases of a-Si surfaces, since it is known that hydrogen can act as a donor in AZO [15]. If the presence of hydrogen coming from the a-Si is the reason for the different electrical properties, the difference of AZO deposited on a-Si:H(i-n) and a-Si:H(i-p) is possibly due to a stronger release of hydrogen for a-Si:H(i-p), as reported by de Wolf [16]. The different release of hydrogen for a-Si:H(i-p), a-Si:H(i-n) and the complete absence of hydrogen for bare glass can also explain the different thermal behavior of AZO, as reported in [1], the presence of hydrogen during annealing can cause higher temperature stability.

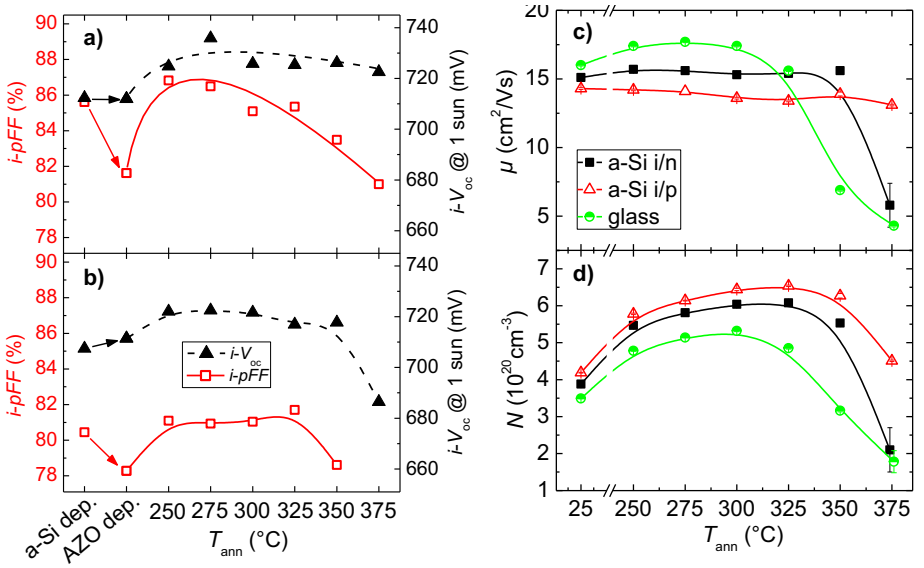

Fig. 5. Annealing temperature dependence of the implied pseudo fill factor (*i-pFF*) and the implied open circuit voltage *i-*V_{oc} of (a) AZO/a-Si(n-i)/c-Si(n)/a-Si(i-n)/AZO hetero BSF and (b) AZO/a-Si(p-i)/c-Si(n)/a-Si(i-p)/AZO hetero emitter structures and the effect on (c) the carrier mobility μ and (d) the carrier concentration N of AZO, the samples were sub sequential annealed for 15 min in oxygen containing atmosphere.

3.3.4. Detailed estimation of the activation energy

In Fig. 6 the natural logarithm of the AZO carrier concentration N over the reciprocal annealing temperature T_{ann} for AZO samples on glass and a-Si coated glass is shown. All annealings were carried out in oxygen containing atmosphere. From so called Arrhenius plots one can estimate the activation energy E_a of the thermal activated donors in AZO, which are summarised in Table 3. The activation energies for AZO on glass or a-Si coated glass are more or less equal, but shifted towards higher carrier concentration for AZO on a-Si coated glass, which is also the case in the test structures in Fig. 3d). In the low temperature range from room temperature to 120 °C, E_a is around 10 meV. This activation energy can be identified as an activation of excitons in neutral donors [13,17]. In the temperature range from 160 to 220 °C E_a is around 54 meV. In literature, an activation energy of 55 meV can be attributed to a formation of Al_{Zn} donors from neutral states [13]. A re-measurement of the 180 °C annealed samples after 20 days storage in air at room temperature under diffuse sun illumination, which corresponds to the points at $2.2 * 10^{-3}$ K^{-1} marked with red arrows, obtains a significant degradation of the carrier concentration. A subsequential performed annealing leads again to an activation of donors with the specific energy of around 55 meV. For temperatures above 250 °C a sharp decrease of the carrier concentration was observed. This deactivation of carriers was reported in the literature as a surface oxidation of AZO [18].

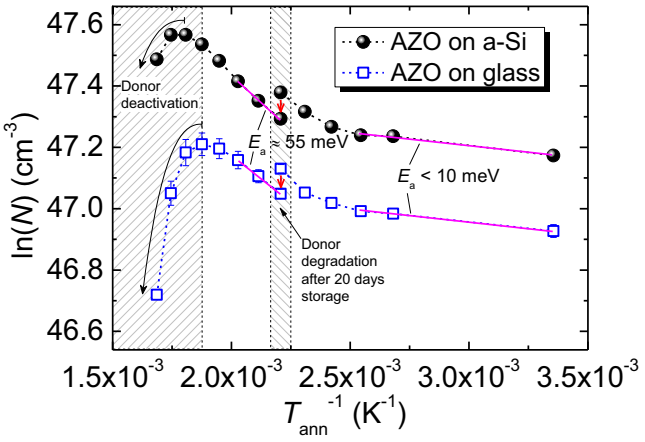

Fig. 6. Natural logarithm of the AZO carrier concentration N over the reciprocal annealing temperature T_{ann} in the range from 25 to 320 °C of samples with AZO on glass and AZO on a-Si coated glass, respectively. The annealing was carried out in oxygen containing atmosphere. The solid lines are linear regressions of data points for the estimation of the activation energy E_a.

Table 3. Calculated thermal activation energies of AZO layers deposited on glass and a-Si(i) coated glass.

Sample structure	E_a (meV) 25 °C < T_{ann} < 120 °C	E_a (meV) 160 °C < T_{ann} < 220 °C
AZO/glass	7	59
AZO/a-Si/glass	7	56

4. Conclusion

It was shown that AZO layers with a thickness below 80 nm deposited at 200 °C obtain good electrical properties, with a carrier concentration N of 2×10^{20} cm^{-3} and a carrier mobility μ up to 20 cm^{2}V^{1}s^{-1} after deposition. The comparison of the electrical parameters of thin and thick AZO layers obtains a limitation especially of the carrier mobility by structural properties, as the grain size of the polymorph material. The annealing of thin AZO layers showed temperature stability up to 450 °C in nitrogen atmosphere, whereas AZO annealed in air starts to deteriorate at 300 °C. The high temperature annealing at 450 °C in an inert gas leads to an improvement of the mobility up to 22 cm^{2}V^{-1}s^{-1}. The presence of a-Si was identified as significant factor on the electrical parameters for as-deposited AZO and its annealing behavior.

Acknowledgements

The authors would like to thank K.U. Ritzau for the inspiring discussions and providing the glass substrates, H. Wernerus for the sample preparations, M. Bivour for the assistance with QSSPC measurements and analysis and our partners in the joint project HERCULES. Funding of the project HERCULES from the European Union's Seventh Programme for research, technological development and demonstration under grant agreement No 608498, is gratefully acknowledged.

References

[1] Yang W, Wu Z, Liu Z, Pang A, Tu YL, and Feng ZC. Room temperature deposition of Al-doped ZnO films on quartz substrates by radio-frequency magnetron sputtering and effects of thermal annealing. Thin Solid Films 519, 2010.
[2] van Sark WGJHM, Korte L, and Roca F. Physics and technology of amorphous-crystalline heterostructure silicon solar cells. Heidelberg, Springer Verlag, 2011.
[3] Schroder DK, Thomas RN, and Swartz JC. Free carrier absorption in silicon. IEEE Transactions on Electron Devices ED-25, 1978.
[4] van der Pauw LJ. A method of measuring specific resistivity and hall effect of discs of arbtrary shape. Philips Research Reports 13, 1958.
[5] Hoff JHvt. Études de dynamique chimique. Amsterdam, Frederik Muller & Co, 1884.
[6] Sinton RA, Cuevas A, and Stuckings M. Proceedings of the 25th IEEE Photovoltaic Specialists Conference, Washington DC, USA, 1996.
[7] Reusch M, Bivour M, Hermle M, and Glunz S. Silicon PV, Hamelin, 2013.
[8] Sinton RA and Cuevas A. Proceedings of the 16th European Photovoltaic Solar Energy Conference, Glasgow, UK, 2000.
[9] Seto JYW. The electrical properties of polycrystalline silicon films. J. Appl. Phys. 12, 1975.
[10] Ma J, Ji F, Zhang D-h, Ma H-l, and Li S-y. Optical and electronic properties of transparent conducting ZnO and ZnO:Al films prepared by evaporating method. Thin Solid Films 357, 1999.
[11] Ellmer K, Mientus, R. Carreir transport in polycrystalline transparent conducting oxides: A comparative study of zinc oxide and indium oxide. Thin Solid Films 516, 2008.
[12] Baker-Finch SC and McIntosh KR. 35th IEEE photovoltaics specialists conference, Honolulu, 2010.
[13] Meyer BK, Alves H, Hofmann DM, Kriegseis W, Forster D, Bertram F, Christen J, Hoffmann A, Straßburg M, Dworzak M, Haboeck U, and A. V. Rodina. Bound exciton and donor–acceptor pair recombinations in ZnO. Phys. Status Solidi B 241, 2004.
[14] Ruske F, Roczen M, Lee K, Wimmer M, Gall S, Hüpkes J, Hrunski D, and Rech B. Improved electrical transport in Al-doped zinc oxide by thermal treatment. Journal of Applied Physics 107, 2010.
[15] Van de Walle CG. Hydrogen as a Cause of Doping in Zinc Oxide. Phys. Rev. Lett. 85, 2000.
[16] De Wolf S and Kondo M. Proceedings of the 4th World Conference on Photovoltaic Energy Conversion, Waikoloa, Hawaii, USA, 2006.
[17] Leem JH. Dependence of the Optical Properties on the Substrate Temperature in ZnO Thin Films Grown on Flexible Polyimide Substrates. J. of the Korean Physical Society 53, 2008.
[18] Studenikin SA, Golego N, and Cocivera M. Carrier mobility and density contributions to photoconductivity transients in polycrystalline ZnO films. J. Appl. Phys. 87, 2000.